

# Large Scale Novel Object Discovery in 3D

Siddharth Srivastava<sup>†</sup>, Gaurav Sharma<sup>‡</sup>, Brejesh Lall<sup>†</sup>

<sup>†</sup> Indian Institute of Technology, Delhi, India, <sup>‡</sup>Indian Institute of Technology, Kanpur, India

eez127506@ee.iitd.ac.in, grv@cse.iitk.ac.in, brejesh@ee.iitd.ac.in

## Abstract

We present a method for discovering never-seen-before objects in 3D point clouds obtained from sensors like Microsoft Kinect. We generate supervoxels directly from the point cloud data and use them with a Siamese network, built on a recently proposed 3D convolutional neural network architecture. We use known objects to train a non-linear embedding of supervoxels, by optimizing the criteria that supervoxels which fall on the same object should be closer than those which fall on different objects, in the embedding space. We test on unknown objects, which were not seen during training, and perform clustering in the learned embedding space of supervoxels to effectively perform novel object discovery. We validate the method with extensive experiments, quantitatively showing that it can discover numerous unseen objects while being trained on only a few dense 3D models. We also show very good qualitative results of object discovery in point cloud data when the test objects, either specific instances or even categories, were never seen during training.

## 1. Introduction

Object discovery has been a popular research area in RGB images [35] and has recently been explored for applicability on 3D data [21, 23]. As humans perceive the world in 3D [26], the ability to reason in 3D becomes a necessary computer vision capability. In the case of autonomous mobile robots, for instance, an important problem is the efficient navigation of the robot in the real world scenario, where inferring and demarcating manipulable objects and their context is one of the main technologies required. Traditionally, such object estimation problem has mostly been well studied in a supervised *known object* scenario [15, 17], i.e. the robot is expected to encounter the same objects it was trained on. However, a more realistic and challenging setting is when the objects that the robot will encounter were never seen before – we address this important problem of discovering never before seen objects from 3D data.

We propose a learning based approach to discover novel

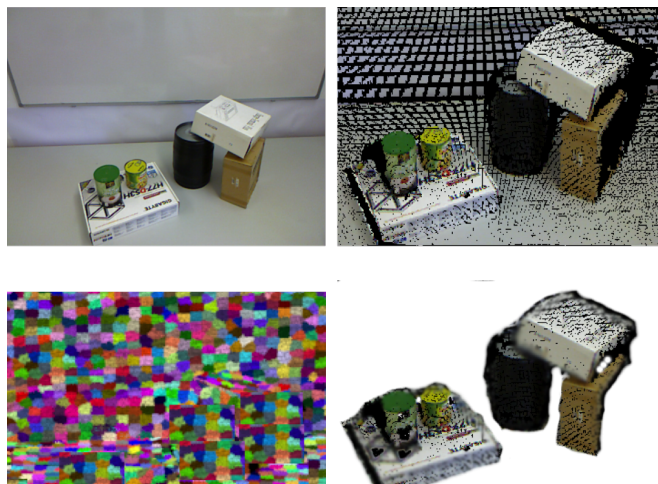


Figure 1: (Left-top) RGB image of a scene containing multiple objects. (Right-top) Point cloud representation of the same scene (noisy). (Left-bottom) Supervoxels obtained from the scene. (Right-bottom) Discovered objects (the point cloud has been post-processed for better illustration)

objects in 3D. The proposed method (i) deals with large scale data, e.g. the number of points processed in the 3D datasets used are of  $\mathcal{O}(10^6)$ , (ii) learns models which have a large number of parameters  $\mathcal{O}(10^5)$  and (iii) discovers objects from approximately 300 unseen object categories. While processing such large scale 3D data, efficiency is a key concern, and the proposed method is successfully able to cope with such scale of both data and models. In our experiments, we show that on a large dataset (with respect to number of classes, models and number of points), earlier techniques lag behind the proposed method. Moreover, with experiments on multiple datasets, we show that the model learned with the proposed method on one (large) dataset, provides state-of-the-art results on other datasets with a standard forward pass on the test point clouds i.e. without need for retraining the network.

We do bottom up aggregation of supervoxels obtained from 3D scenes into objects. We work in the setting where at test time, on the field, the robot would encounter novel objects which were never seen while training. The novel

perspective comes from the use of discriminative metric learning approach for obtaining the similarity between supervoxels which are expected to belong to the same object, which might itself be unknown. There have also been recent attempts to find 3D bounding boxes around objects, e.g. generic object proposals in 3D [6, 33]. Here, we aim at discovering strict object boundaries in 3D, and not just bounding boxes, which could help, e.g., in better grasping by a robot. Borrowing from the recent success of deep learning based methods on (i) 3D data [5, 9, 22, 36, 38], (ii) non-linear embeddings, on various computer vision problems, e.g. face verification [30], face retrieval [4], semantic image retrieval [31], and (iii) unsupervised feature learning [19, 37], we propose to use a deep Siamese network for the task of learning non-linear embeddings of supervoxels into a Euclidean space, such that the  $\ell_2$  distances in the embedding space reflect object based similarities.

In summary, we address the problem of 3D object discovery in a supervised, but constrained setting where we are given a few known objects at train time, while, at test time we are expected to discover novel unknown objects. We train a 3D-CNN using voxelized CAD models, and use supervoxels at multiple resolutions to learn a distance metric among supervoxels that are similar (same object) and distinct (different objects). The contributions of this paper are as follows. (i) We propose a Siamese network based embedding learning framework for supervoxels which works directly with point cloud data and can be trained end-to-end, (ii) the proposed method is fast, requiring three sub-steps of (a) supervoxel computation, (b) a CNN forward pass and (c) classification of supervoxels with learned discriminative embeddings, (iii) we show with quantitative and qualitative results, on challenging public datasets of 3D point clouds, that the structure of objects in terms of distances between supervoxels can be learned from only a few reference models and can be used to generalize to (supervoxels of) unseen objects, (iv) while previous object discovery methods were evaluated on a small number of distinct objects ( $2 \sim 10$ ), we show that the proposed technique can efficiently detect objects from a large number of classes and object instances per class ( $\sim 100$  and  $\sim 200$  respectively), (v) we show improvements w.r.t. challenging baselines and report state-of-the-art results on three public benchmarks, namely NYU Depth v2, Object Discovery Dataset, and Object Segmentation Dataset, on the task of novel object discovery in 3D point cloud data.

## 2. Related Work

The general pipeline followed by the majority of the works related to object discovery in 3D is shown in Fig. 2. Among the representative works, Karpathy et al. [21] discover objects by using multiple views from a 3D mesh. Garcia et al. [12] generate object candidates by over-

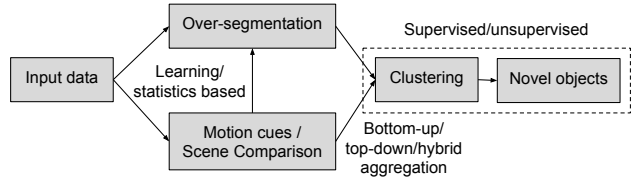


Figure 2: General Pipeline of Object Discovery Methods

segmenting the RGB-D images. They then fuse the segments, obtained using Voxel Cloud Connectivity Segmentation (VCCS) [25], with various ranking criterion, to obtain discovered objects. Compared to these works, we apply discriminative metric learning to learn which segments should be fused. Meuller et al. [23] first over-segment the RGB-D point cloud and then learn a classifier for primitive objects. The approach is similar to ours but in our method, we do not explicitly assume any structural composition of basic shapes that constitute an object, allowing us to deal with more complex and novel object categories. Richtsfeld et al. [27] perform object discovery on the constrained domain of table-top scenes. Firman et al. [11] learn similarity among segments of an image by training a classifier as well, while our features are learned using a deep convolutional network trained on CAD models and we learn the similarity and dissimilarity among segments (supervoxels) with a supervised metric learning based objective.

Authors in [18] propose to discover objects by determining frequently occurring object instances and determining the patches that move in the scenes. Shin et al. [32] find repetitive objects in 3D point clouds by forming superpixel like segments of points based on relation between normals of neighbouring points. As a limitation, they can only find objects which are repeated in a dataset as their method is based on finding multiple occurring segments. We overcome this limitation by learning the discrimination measure among supervoxels belonging to same and distinct objects.

Bao et al. [3] perform attention driven segmentation by detecting a salient object using depth information and then forming a 3D object hypothesis based on the shape information. They label and refine objects using Markov Random Field in voxel space with constraints of spatial connectivity and correlation between color histograms. Stein et al. [7] decompose a scene into patches while categorizing edges as convex or concave and thus creating a locally connected sub-graph. Their technique is unsupervised but mostly detects object parts instead of complete objects. Gupta et al. [16] perform segmentation based on an object’s geometric features such as pose and shape. Asif et al. [2] propose perceptual grouping of segments based on geometric features. Collet et al. [8] develop a graph based approach incorporating metadata such as prior knowledge about objects, environments etc. for discovering objects from raw RGB-D data streams. While most of the previous methods cater to in-

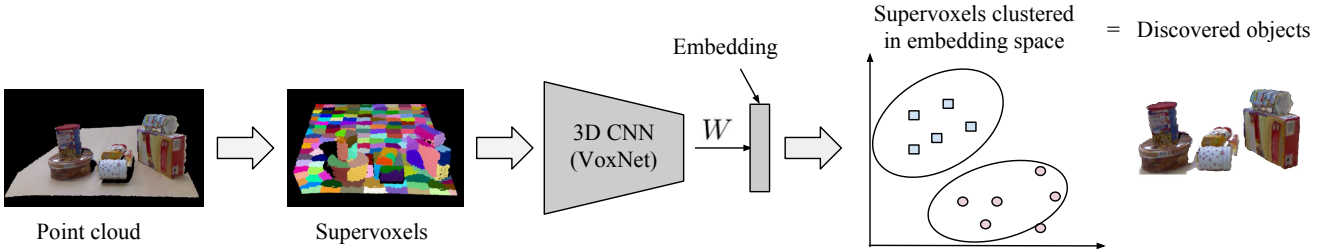


Figure 3: Block diagram of the proposed approach at test time. The 3D convolutional network used to embed the supervoxels is trained using a Siamese network which captures object based similarity of the supervoxels. See Sec. 3 for details.

door scenes, Zhang et al. [39] tackle the problem of discovering category in an urban environment. They pose object discovery as a problem of determining category structures by finding repetitive patterns of shape and refining the segmentations by defining an energy function which minimizes distances between the shape patterns.

### 3. Approach

We now describe our approach for discovering objects in 3D point cloud data. Fig. 3 gives the overall block diagram of the approach at test time. At training time the 3D convolutional neural network is trained in a specific manner which we explain below. We obtain point cloud data from an appropriate sensor, e.g. Microsoft Kinect. The overall strategy is then to discover novel objects in 3D by clustering supervoxels obtained from the point cloud of a scene. To obtain the distance metric required for clustering, we propose to use deep Siamese network for learning non-linear embeddings of supervoxels into a Euclidean space, where the distance reflects the object membership, i.e. the supervoxels which belong to the same object are closer than those which belong to different objects. Learning such a distance metric requires supervised training data, which we obtain from (the point cloud data of) a set of few known objects. Note that while the proposed method requires annotated training data, the data it uses is not from the objects it will see at test time, i.e. at test time the method is expected to discover novel objects which it had not seen during training. Hence, the method is different from the traditional object detection methods which aim to find the objects, which they were trained on. Finally, when we have the object based supervoxel embedding, we perform clustering using an efficient method to obtain object hypothesis. We now explain each component in complete detail.

#### 3.1. Oversegmentation using Supervoxels

The first step of our method involves obtaining an oversegmentation of the 3D data using supervoxels. Towards that goal, we use an efficient and robust method to deal with the noisy and large amount of point cloud data. We group the points in the point clouds into supervoxels using Voxel

Cloud Connectivity Segmentation (VCCS) approach of Papon et al. [25]. Since (i) the number of points in the point clouds are very large,  $\mathcal{O}(10^6)$ , and (ii) they are noisy as well, this first step of supervoxelization, reduces the computational load on the successive stages and also lends robustness against noise. Since the objective optimized by the supervoxels creation method is that they should not cross object boundaries, we aim to thus cluster these supervoxels to give us plausible novel objects at test time. The seed resolution used to construct supervoxels describes the fineness (low seed resolution) or coarseness (high seed resolution) of the supervoxel segmentation, allowing us to have multi-scale supervoxels that can capture fine details as well as larger blocks of the objects of interest. Hence, we extract supervoxels at multiple seed resolutions and later merge them appropriately as described below for coherent object hypotheses.

#### 3.2. Siamese Deep Network

As the next component, we learn a similarity metric which captures object based distances between the supervoxels, i.e. it brings those on the same object closer while pushing those on different objects far. To do this, we employ a Siamese network which learns a non-linear embedding into a Euclidean space where the distance captures such semantic relation between the supervoxels.

Now, we first outline how we utilize the supervoxels, generated above, with the Siamese network and then describe the network architecture, loss function as well as training procedure in detail.

Once we have the supervoxels from the point cloud data, we generate ‘positive’ and ‘negative’ pairs (for each seed resolution) for training the Siamese network as follows. To generate the positive pairs of supervoxels, we consider all the objects that are labelled during training. For all the supervoxels  $\{z_i | i = 1, \dots, N\}$ , in the training set, we create two sets containing all possible pairs of supervoxels of the following two kinds respectively, (i) the two supervoxels lie on the same object ( $S_+$ ) or (ii) they lie on different objects or background ( $S_-$ ). To decide if a supervoxel  $z_i$  lies in an object  $x \in X$  (with  $X$  being the set of all objects in the current scene) or not, we take the intersection of the points

$z_i$  with the set of points lying on the object  $x$ . If the fraction of these points is more than a threshold  $\beta \in \mathbb{R}$ , of the total number of points in the supervoxel, then it is considered to lie on the object. Note that by doing this we are, effectively, not doing a hard assignment where the supervoxel is required to lie completely in the object, but doing a soft assignment where the supervoxel is required to be sufficiently inside the object. Similarly, the set,  $S_-$ , of negative pairs contains supervoxels which do not belong to the same object, i.e. they either belong to two different objects or to an object and to the background, respectively. More details on selecting supervoxels on object and background for training the network are provided in Sec. 4. The following equation formalizes this mathematically.

$$\begin{aligned} &\forall i, j \in [1, N], i \neq j \\ &(z_i, z_j) \in S_+ \quad \text{iff, } \exists x \in X \text{ s.t.} \\ &\frac{|pts(z_i) \cap pts(x)|}{|pts(z_i)|} \geq \beta \text{ and } \frac{|pts(z_j) \cap pts(x)|}{|pts(z_j)|} \geq \beta, \\ &(z_i, z_j) \in S_- \text{ otherwise} \end{aligned} \quad (1)$$

where,  $pts(t)$  gives the set of points in the object  $t$  and  $|\mathcal{A}|$  denotes cardinality of the set  $\mathcal{A}$ .

Given such pairs of same and different object supervoxels, we proceed to train the Siamese network. Our Siamese network is based on the recently proposed convolutional neural network for 3D point cloud data by Maturana and Scherer, called VoxNet [22]. VoxNet takes the point cloud as input, computes the occupancy grid with it and transforms it using two convolutional layers, a max pooling layer and finally a fully connected layers to finally perform classification over a predefined number of objects. While it was proposed for object classification in 3D we use it for processing supervoxels for obtaining their semantic non-linear embeddings. We have two parallel streams of the VoxNet, with tied parameters, which take the two members of the positive (or negative) pair and do a forward pass up to the last fully connected layer (removing the final classification layer). On top of the last fully connected layer from the two streams, we put a loss layer based on the hinge loss for pairwise distances given by,

$$\mathcal{L}(\Theta, W) = \sum_{S_+ \cup S_-} [b - y_{ij}(m - \|Wf_{\Theta}(z_i) - Wf_{\Theta}(z_j)\|)^2]_+ \quad (2)$$

where,  $[a]_+ = \max(a, 0) \forall a \in \mathbb{R}$ .

The VoxNet forward pass, parametrized by  $\Theta$ , is denoted by  $f_{\Theta}(\cdot)$ ,  $W$  is the parameter of the projection layer after VoxNet,  $(z_i, z_j)$  is the pair of supervoxels and  $y_{ij} = +1$  or  $-1$  indicates if they are from the same or different objects, i.e. if the pair belongs to  $S_+$  or  $S_-$ , respectively.  $b \in \mathbb{R}$  and  $m \in \mathbb{R}^+$  are bias and margin hyper-parameters respectively.

The loss effectively ensures that in the embedding space obtained after the forward pass by VoxNet and the projec-

tion by  $W$ , the distances between positive pairs are less than  $b - m$ , while those between the negative pairs are greater than  $b + m$ . When trained on the given train objects, we expect the loss to capture the semantic distances between the supervoxels in general, which would then generalize to supervoxels of novel unknown objects at test time. As we show in the empirical results, we find this to be indeed the case.

### 3.3. Supervoxel Clustering and Postprocessing

Once we have trained the Siamese network, we can embed the supervoxels into a object based semantics preserving Euclidean space. We then perform clustering in this space to obtain novel object hypotheses. We use DBSCAN [10] to group similar supervoxels into larger segments. DBSCAN clusters the supervoxels based on density i.e. distribution of nearby supervoxel features. As the features are learned by the deep siamese network to be closer in the embedding space if they belong to same object, they are considered as potential neighbours by DBSCAN and vice-versa for those which do not belong to the same object.

We observe that most of the objects were spanned by multiple supervoxels, especially since the supervoxels were extracted at multiple scales. Therefore, the criteria for a dense region in DBSCAN was specified as at least two supervoxels in size. This limits the method to discover objects that consist of at least two supervoxels. In our experiments, we did not find any object with single supervoxel in the training set, but we do note that in the real world where a robot is navigating, a single supervoxel may possibly correspond to a heavily occluded object. But it would be important to note that in case of robot navigation, detecting such heavy occlusions is not a problem since the the object occluding the view needs to be processed first before moving on to the object behind it. Moreover, in such cases there are chances that the visible patch of the occluded object becomes a part of another object. As we show in experiments, the proposed technique is very robust to such patches and avoids intermixing beyond object boundaries.

## 4. Experimental Results

**Datasets.** We show results on the following challenging and publicly available datasets.

*NYU Depth v2* [24]: The dataset consists of 1449 RGB-D images with 894 classes and 35064 object instances. We use this dataset to create a challenging test setting for object discovery. This is in contrast to most of the previous works where evaluation was done on much smaller datasets consisting of only a few hundred object instances belonging to only a few classes.

*Universal Training Dataset:* We create a training set from NYU Depth v2 dataset with 60% of the classes. We use this as the universal training set for all the experiments

reported in this paper. We ensure that none of the objects in evaluated test datasets have been seen before. We note explicitly here that the *Universal Training Dataset* does not contain any class that are present in any of the test data. During testing we only use test split of the corresponding datasets and report results on them, except for NYU Depth v2 where we use the remaining classes (and instances) for testing. As a scene in NYU Depth v2 consists of multiple classes and its instances, any object belonging to the test class is labelled as clutter/background in the training set.<sup>1</sup>

*Object Discovery dataset* [23]: The dataset consists of 30 RGB-D scenes with  $640 \times 480$  resolution. There are total 296 objects where 168 are categorized as simple-shaped and 128 as complex-shaped.

*Object Segmentation dataset* [1, 27]: The dataset consists of 111 scenes categorized into six subsets i.e. Boxes, Stacked Boxes, Occluded Objects, Cylindrical Objects, Mixed Objects and Complex Scenes. The dataset provides a train/test split of 45 and 66 point clouds respectively. We used the test set as provided by the authors with the dataset.

**Baselines.** We report results with two baselines. The first baseline uses keypoint based 3D descriptors while the second is an extended deep architecture based on VoxNet.

*3D keypoint based descriptors.* We generate supervoxels from the *Universal Training Dataset* and extract various descriptors for points in each supervoxel. The cumulative feature descriptor of the supervoxel is calculated by using average pooling and max pooling of descriptors. The positive and negative pairs of ground-truth data are prepared using the same method as described earlier. We then utilize DBSCAN to find clusters of supervoxels which we mark as discovered objects. The evaluated descriptors are Signatures of Histograms of Orientations (SHOT) [29, 34], Fast Point Feature Histograms [28], Rotational Projection Statistics (RoPS)[14] and Spin Image (SI) [20] for their superior performance on various metrics for 3D computer vision tasks [13]. These make for very competitive baselines with traditional hand-crafted 3D descriptors.

*Deep VoxNet Classification (DVC) Network.* We remove the last layer of the original VoxNet and append two fully connected layers followed by a multiclass classification layer. This method basically classifies each of the training supervoxel into one of the training classes. At test time we pass each of the supervoxel through the network and keep the last fully connected layer responses as the features of the supervoxels. These supervoxel features are then clustered using DBSCAN clustering. This baseline allows us to evaluate the advantages obtained, if any, by using the pro-

<sup>1</sup>We tried to take only images with the train objects and no test class objects but could not create a big enough training set, hence we resorted to the current setting. In our training set while some of the test objects may be present, they are not annotated (marked as background) and are never used for the supervised training.

posed Siamese method.

**Comparison and evaluation setup.** On NYU Depth v2 dataset, we compare our results against Stein et al. [7], Silberman et al. [24], and Gupta et al. [16]. The first one is an unsupervised segmentation technique while the latter two involve prior training. The technique of Gupta et al. is related to semantic segmentation in 3D, and is compared here because it reports good performance on NYU Depth v2 and to evaluate if such techniques can be used for the task of object discovery, i.e. when the training and testing set contain mutually exclusive object categories. Accuracy is computed by counting the number of objects where the discovered clusters have greater than 80% point-to-point overlap with the ground truth for classes not in the *Universal Training Dataset*. The over-segmentation ( $F_{os}$ ) and under-segmentation ( $F_{us}$ ) rates are computed using the method defined in [27] and are given by Eq. 3 where  $n_{true}$ ,  $n_{false}$  and  $n_{all}$  are number of correctly classified, incorrectly classified and total number of object points in a point cloud.

$$F_{os} = 1 - \frac{n_{true}}{n_{all}}, F_{us} = \frac{n_{false}}{n_{all}} \quad (3)$$

We store a mapping of ground-truth labels of points in point cloud to that of supervoxel and further in the voxelized cloud. We use these mappings once the supervoxels have been clustered to obtain  $n_{true}$  and  $n_{false}$ .

On Object Discovery Dataset, the evaluation metrics used are as defined in [23], which are, over-segmentation ( $r_{os}$ ), under-segmentation ( $r_{us}$ ), good-segmentation ( $r_{gs}$ ) and mis-segmentation ( $r_{ms}$ ) rates to evaluate various methods on this dataset computed by using labelled segments of object parts. Instead of using object parts, we consider each object as a segment for comparison on this dataset, which is a more stringent requirement since the discovered segments need to correspond to the entire object instead of object parts. The good-segmentation rate is computed by finding the largest point to point overlap among ground truth and detected objects, while any clusters partially overlapping with the ground truth objects, contribute to the over-segmentation rate. The points in ground-truth object which do not belong to any discovered cluster are considered as mis-segmentations. For remaining discovered clusters, the overlap is calculated with ground-truth clusters, among those the largest overlap cluster is ignored (as they have already been considered), while the rest contribute to mis-segmentation rate.

**Training details.** We train the VoxNet using the implementation corresponding to [22] on ModelNet10 and ModelNet40 [38] voxelized datasets. We then use this pre-trained VoxNet model with the proposed Siamese architecture.

Discriminative Metric Learning is performed on top of VoxNet as follows. We use the *Universal Training Dataset*

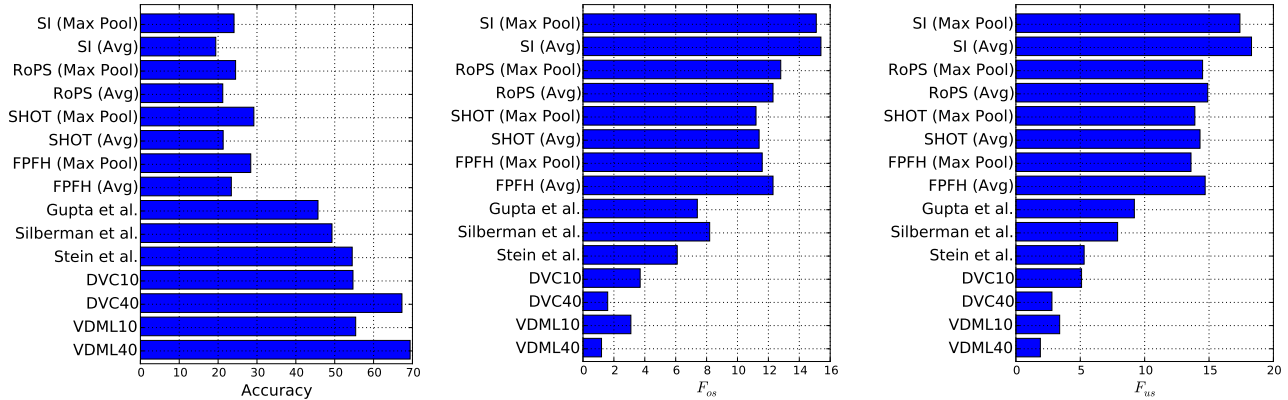


Figure 4: Accuracies,  $F_{os}$  and  $F_{us}$  scores on NYU Depth v2 dataset. Lower is better for  $F_{os}$  and  $F_{us}$  scores.

described previously for training the Siamese network using discriminative metric learning. The supervoxels are extracted with seed resolutions of 0.05m, 0.10m, 0.15m and 0.2m and subject to the constraint that the % of ground-truth object points in the supervoxel should be greater than or equal to a threshold  $\beta$ . We use the value of  $\beta = 0.8$ . The value allows for soft-assignment of supervoxels as positive pairs and was chosen based on empirical evaluation described later (Sec. 4.1). The positive set of supervoxels is constructed by pairing all supervoxels on the same object for every object in the training data. The negative set consists of two types of supervoxel pairs. First are the supervoxels belonging to different objects, for this we only use supervoxels around the center of the objects to avoid confusion around boundaries, and second are the pairs of neighbouring supervoxels at object boundaries. We also add pairs of supervoxels belonging to the background classes to the negative set (wall, floor etc.), considering them to contribute to hard negatives as they potentially come from very similar objects.

**Testing details.** The test set consists of remaining 40% classes of the NYU Depth v2 dataset. The results are reported on classes in test set only even if some of the test scenes may contain classes from training set, this may occur since NYU Depth v2 consists of real world complex scenes and having a clean separation of images with train only and those with test only objects was found to be infeasible.

#### 4.1. Quantitative Results

The results for proposed VoxNet with Discriminative Metric Learning (VDML) on NYU Depth v2 along with the baselines described above are shown in Fig. 4. VDML outperforms other methods, achieving 55.4% and 69.4% test set accuracy on ModelNet10 (VDML10) and ModelNet40 (VDML40) trained 3D-CNN respectively. It is closely followed by DVC with a test set accuracy of 54.7% and 67.3% on ModelNet10 (DVC10) and ModelNet40 (DVC40) re-

spectively. Even training VoxNet with ModelNet10, we observe that the accuracy is nearly the same as the DVC baseline while being significantly higher than other baseline methods where the mean performance of descriptors with average pooling is 21.3% while that of max-pooling is 26.6%. Another advantage of VDML over DVC is lower training time. During our experiments, it took 60% more time to train DVC as compared to VDML. This can be explained by the presence of additional fully connected layers in DVC. Compared to Stein et al., VDML40 achieves 14.9% higher accuracy while method of Silberman et al. and Gupta et al. lag behind by 20.1% and 23.7% respectively. This shows that VDML although following supervised approach is able to generalize better on unseen objects in complex scenes.

Fig. 4 also shows over-segmentation ( $F_{os}$ ) and under-segmentation ( $F_{us}$ ) scores. The  $F_{os}$  for VDML10 and VDML40 are 3.1% and 1.2% respectively. The corresponding values for DVC10 and DVC40 are 3.7% and 1.6% respectively. Comparatively, DVC has higher under-segmentation (5.1% for DVC10 and 2.8% for DVC40) than VDML (3.4% for VDML10 and 1.9% for VDML40). The low  $F_{os}$  and  $F_{us}$  demonstrate that VDML results in lower cross-overs on object boundaries in segmented regions. The other baselines except DVC perform poorly while methods of Stein et al., Silberman et al. and Gupta et al. perform average with  $F_{os}$  being 6.1%, 8.2% and 7.4% respectively. An interesting point to note is the significant reduction in  $F_{os}$  and  $F_{us}$  scores when compared to training on ModelNet10 and ModelNet40 respectively. It shows that when the methods are provided with larger number of models, the resulting features are able to better characterize and learn object boundaries in the embedding space. This underlines the need for more training data in the 3D domain.

The results on Object Discovery Dataset are shown in Table 1. As can be seen in the results, the proposed method VDML achieves a good-segmentation rate ( $r_{os}$ ) of 98.1% on all objects which is a higher by 5.2% when compared

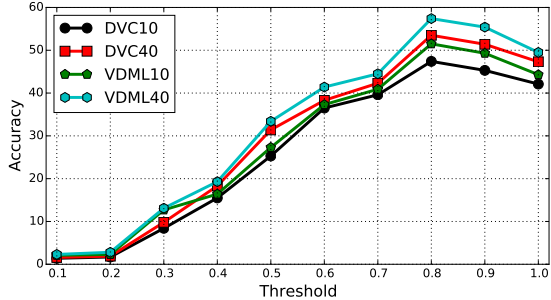


Figure 5: Accuracy vs. threshold of supervoxel overlap with ground-truth for training on NYU Depth v2 dataset.

to best performing technique (CPC) in [23]. It would be interesting to note that we obtain significantly reduced over-segmentation ( $r_{os} = 3.2$ ) and under-segmentation ( $r_{us} = 1.7$ ) rates on all objects demonstrating that the discovered objects are closer to the complete objects. The mis-segmentation rate, though, is reduced primarily due to background clutter in a few scenes which are not present as ground-truth labels in the training set.

The results on Object Segmentation Dataset are shown in Table 2. We achieve a test set accuracy of 99.24% which is 0.83% higher than  $SVM_{nmb}$  and 11.2% than  $SVM_{nb}$  of [27]. Interestingly, we achieve 100% accuracy on point clouds with geometrically simpler Boxes and Stacked Boxes objects, while also having very low, 0% over-segmentation and 0.1% under-segmentation rates. These values become more significant when compared to  $SVM_{nmb}$  where higher accuracy is accompanied by significantly large under-segmentation rates i.e. 17.2% and 28.2% as compared to VDML40 with 0.1% and 4.4% on boxes and stacked boxes respectively. The  $F_{us}$  rate on complex objects for VDML40 is 4.24% while that for  $SVM_{nmb}$  and  $SVM_{nb}$  are 146% and 8.0% respectively.  $SVM_{nmb}$  witnesses large under-segmentation rate as it is more sensitive to connection between neighbouring segments. On the other hand, VDML is trained on multiple seed resolutions of supervoxels allowing it to learn more intricate connectivity patterns among supervoxel boundaries and hence prevent it from connecting entire objects if a few segments (supervoxels) are incorrectly assigned to the same object.

**Impact of ground-truth overlap threshold.** Fig. 5 shows the variation in accuracy vs. threshold ( $\beta$ ), for percentage of points that overlap with ground-truth, to consider it as a positive supervoxel for training. The graph was obtained by splitting the train dataset into train and validation sets with a ratio of 80% to 20% respectively and performing 5-fold cross-validation. It can be observed that the accuracy reaches a peak at 0.8 for both DVC and VDML trained on either of ModelNet10 or ModelNet40. An explanation of better performance of soft supervoxel assignment is because the generated supervoxels do not always lie perfectly within

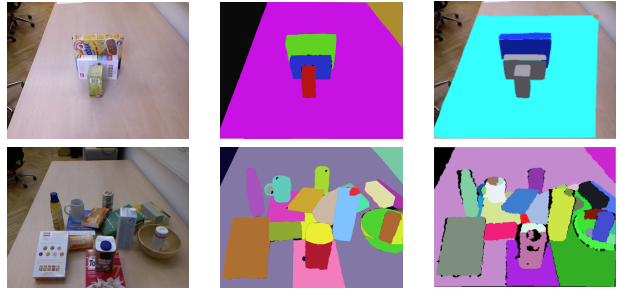


Figure 6: Qualitative results from Object Segmentation Dataset. First column shows the original images, second column shows the result using VDML40, while the third column shows results using [27] and [7] respectively.

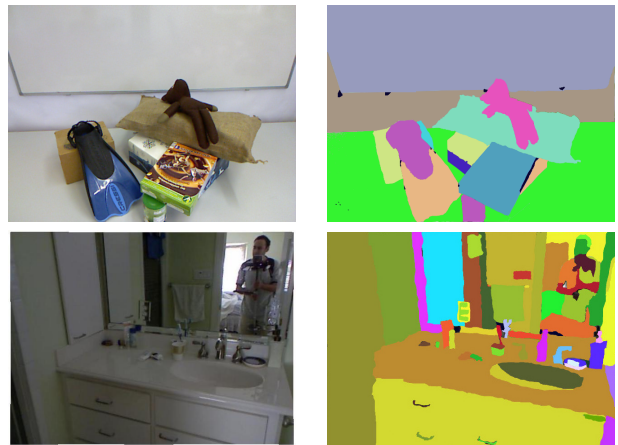


Figure 7: Left column has the original images while the right one shows the discovered objects using VDML40 from Object Discovery Dataset and NYU Depth v2 resp.

object boundaries. A hard assignment would therefore result in rejection of many supervoxels near the object boundaries. Since our method maximizes the distance between supervoxels on boundaries and neighbouring supervoxels (on background or other objects), a hard assignment has a negative impact on the overall performance which is also validated by a drop of 7.2% and 7.9% (hard-assignment) in accuracy as compared to soft-assignment ( $\beta = 0.8$ ) on validation set with VDML10 and VDML40 respectively. On the other hand, despite having lower validation set accuracy (and subsequently on test set also) DVC witnesses a lower drop of 5.3% (DVC10) and 6.2% (DVC40) as compared to VDML. This demonstrates that it is relatively less prone to supervoxel assignment criteria c.f. the proposed VDML.

## 4.2. Qualitative Results

Fig. 6 shows visual comparison of results from Richtsfeld et al. [27] and Stein et al. [7] on Object Segmentation.

<b>T</b>	<b>Simple-shaped</b>					<b>Complex-shaped</b>					<b>All Objects</b>				
<i>N</i>	168					128					296				
<i>S</i>	APS	SPS	SPC	CPC	V40	APS	SPS	SPC	CPC	V40	APS	SPS	SPC	CPC	V40
$r_{os}$	92.3	43.9	6.6	4.3	2.1	93.1	51.3	22.3	2.8	1.7	92.7	48.8	14.3	4.1	3.2
$r_{us}$	2.4	1.6	1.9	3.7	2.9	1.3	0.9	0.8	0.8	0.5	1.7	1.4	1.6	2.6	1.7
$r_{gs}$	6.8	55.2	92.5	92.3	97.8	6.3	48.1	77.1	94.5	98.3	6.6	50.5	84.9	92.9	98.1
$r_{ms}$	0.8	0.8	0.8	3.4	0.4	0.6	0.6	0.6	2.7	1.6	0.7	0.7	0.7	2.9	1.1

Table 1: Comparison on Object Discovery Dataset. Values of APS, SPS, SPC and CPC are from [23], V40 refers to VDML40, T = Type of Dataset, N = number of objects, S= Segmentation Technique and rates  $r_{os,us,gs,ms}$  in percentage.

<b>Technique</b>	<b>SVMnb</b>			<b>SVMnmb</b>			<b>VDML40</b>		
	Acc.	$\bar{F}_{os}$	$\bar{F}_{us}$	Acc.	$\bar{F}_{os}$	$\bar{F}_{us}$	Acc.	$\bar{F}_{os}$	$\bar{F}_{us}$
Boxes	88.55	1.8	0.2	98.19	0.2	17.2	100.0	0.0	0.1
Sta. Box.	89.15	1.3	7.1	98.99	0.0	28.2	100.0	0.0	4.4
Occ. Obj.	87.93	16.6	0.1	99.23	0.0	0.2	99.96	0.08	0.1
Cyl. Obj.	91.66	2.6	0.3	96.77	2.6	3.5	99.3	0.7	0.9
Mix. Obj.	91.04	1.9	19.7	94.97	1.3	1.3	98.5	0.6	1.7
Com. Obj.	84.61	7.0	8.0	98.97	5.4	146	97.7	2.3	4.2
Total	87.72	4.5	7.9	98.41	2.7	69.5	<b>99.24</b>	<b>0.61</b>	<b>1.9</b>

Table 2: Comparison with [27] on Object Segmentation Dataset.

tion Dataset. In Fig. 6 (c), the technique of [27] tends to show under-segmentation and discovers two distinct objects as a single object (grey). In comparison, VDML is able to clearly distinguish among those objects. In Fig. 6 (second row), we compare our approach on a scene with numerous occluded objects. Fig. 6 (f) shows the results provided by Stein et al. [7]. On comparing Fig. 6(e) and 6(f), it can be seen that VDML results in lesser number of points classified as clutter (shown in black) while providing smoother boundaries which would be helpful for applications such as robot grasping. In both the cases, the can at the front suffers over-segmentation. In the first case, there are two visually arbitrary segments while in the case of the proposed VDML those segments correspond to the body of the can and top of the can. Moreover, the segments from the proposed VDML are closer to the ground-truth as less number of points are marked as clutter.

Fig. 7 (first row) shows results of our segmentation on Object Discovery Dataset. There are two important observations to make here. First, as above, the boundaries are closer to the ground-truth. This shows that VDML has learned to distinguish between object and non-object boundaries since the training procedure explicitly focussed on supervoxel pairs around the object boundaries. Secondly, we observe over-segmentation in the object towards the left in Fig 7 (b) –the object gets divided into two segments. Although, we note that the two segments actually belong to visually dissimilar parts of an object, which can easily be considered as distinct objects in the absence of any context.

Fig. 7 (second row) shows results on NYU Depth v2 dataset. Since the previous visual images consisted of objects of relatively similar sizes, we now demonstrate the results on scenes with larger variation in sizes of objects. For example, the demonstrated image consists of objects like a soap as well as a human. It can be observed that VDML is able to clearly distinguish among the objects in front of the mirror (Fig. 7 (d)) except the bottles, where we observe over-segmentation. The wash-basin also gets over-segmented, possibly due to variation in depth and illumination across its surface. Although the objects in the mirror are difficult to discover due to lack of variation in depth, VDML still obtains distinguishable boundaries among various objects (towel, curtain) while over-segmenting the person holding the camera.

## 5. Conclusion

We proposed a novel object discovery algorithm which operates in the challenging learning based setting where the objects to be discovered at test time were never seen at train time. We used recent advances in 3D Convolutional Neural Networks and built on it a Siamese deep network for learning non-linear embeddings of supervoxels into a Euclidean space which reflects object based semantics. In the embeddings space the supervoxels from the same objects were constrained to be closer than the supervoxels from different objects. Once these embeddings are learned they can be used with supervoxels of different novel classes for doing object discovery using efficient clustering in the embedding space. We used a hybrid approach of using CAD models and subsequently RGB-D images for learning non-linear embeddings of supervoxels for discovering objects that were never seen before. We provided comprehensive empirical evaluation and comparison with several baselines and existing methods to demonstrate the effectiveness of the technique. We showed that the proposed architecture achieves high accuracy with low over and under segmentation rates making it more reliable in the context of competing methods. We also demonstrated qualitatively the improved performance of the proposed method.



## References

- [1] Andreas richtsfeld. the object segmentation database (osd). <http://www.acin.tuwien.ac.at/?id=289>. Accessed: 2017-01-06.
- [2] U. Asif, M. Bennamoun, and F. Sohel. Unsupervised segmentation of unknown objects in complex environments. *Autonomous Robots*, 40(5):805–829, 2016.
- [3] J. Bao, Y. Jia, Y. Cheng, and N. Xi. Saliency-guided detection of unknown objects in rgb-d indoor scenes. *Sensors*, 15(9):21054–21074, 2015.
- [4] B. Bhattarai, G. Sharma, and F. Jurie. CP-mtML: Coupled projection multi-task metric learning for large scale face retrieval. In *CVPR*, 2016.
- [5] S. Bu, Z. Liu, J. Han, J. Wu, and R. Ji. Learning high-level feature by deep belief networks for 3-d model retrieval and recognition. *IEEE Transactions on Multimedia*, 16(8):2154–2167, 2014.
- [6] X. Chen, K. Kundu, Y. Zhu, A. G. Berneshawi, H. Ma, S. Fidler, and R. Urtasun. 3d object proposals for accurate object class detection. In *Advances in Neural Information Processing Systems*, pages 424–432, 2015.
- [7] S. Christoph Stein, M. Schoeler, J. Papon, and F. Worgotter. Object partitioning using local convexity. In *Proceedings of the IEEE Conference on Computer Vision and Pattern Recognition*, pages 304–311, 2014.
- [8] A. Collet, B. Xiong, C. Gurau, M. Hebert, and S. S. Srinivasa. Herdisc: Towards lifelong robotic object discovery. *The International Journal of Robotics Research*, 34(1):3–25, 2015.
- [9] A. Eitel, J. T. Springenberg, L. Spinello, M. Riedmiller, and W. Burgard. Multimodal deep learning for robust rgb-d object recognition. In *Intelligent Robots and Systems (IROS), 2015 IEEE/RSJ International Conference on*, pages 681–687. IEEE, 2015.
- [10] M. Ester, H.-P. Kriegel, J. Sander, X. Xu, et al. A density-based algorithm for discovering clusters in large spatial databases with noise. In *Kdd*, volume 96, pages 226–231, 1996.
- [11] M. Firman, D. Thomas, S. Julier, and A. Sugimoto. Learning to discover objects in rgb-d images using correlation clustering. In *2013 IEEE/RSJ International Conference on Intelligent Robots and Systems*, pages 1107–1112. IEEE, 2013.
- [12] G. M. García, E. Potapova, T. Werner, M. Zillich, M. Vincze, and S. Frintrop. Saliency-based object discovery on rgb-d data with a late-fusion approach. In *2015 IEEE International Conference on Robotics and Automation (ICRA)*, pages 1866–1873. IEEE, 2015.
- [13] Y. Guo, M. Bennamoun, F. Sohel, M. Lu, J. Wan, and N. M. Kwok. A comprehensive performance evaluation of 3d local feature descriptors. *International Journal of Computer Vision*, 116(1):66–89, 2016.
- [14] Y. Guo, F. Sohel, M. Bennamoun, M. Lu, and J. Wan. Rotational projection statistics for 3d local surface description and object recognition. *International journal of computer vision*, 105(1):63–86, 2013.
- [15] S. Gupta, P. Arbeláez, R. Girshick, and J. Malik. Indoor scene understanding with rgb-d images: Bottom-up segmentation, object detection and semantic segmentation. *International Journal of Computer Vision*, 112(2):133–149, 2015.
- [16] S. Gupta, P. Arbeláez, and J. Malik. Perceptual organization and recognition of indoor scenes from rgb-d images. In *Proceedings of the IEEE Conference on Computer Vision and Pattern Recognition*, pages 564–571, 2013.
- [17] S. Gupta, R. Girshick, P. Arbeláez, and J. Malik. Learning rich features from rgb-d images for object detection and segmentation. In *European Conference on Computer Vision*, pages 345–360. Springer, 2014.
- [18] E. Herbst, P. Henry, X. Ren, and D. Fox. Toward object discovery and modeling via 3-d scene comparison. In *Robotics and Automation (ICRA), 2011 IEEE International Conference on*, pages 2623–2629. IEEE, 2011.
- [19] C. Huang, C. Change Loy, and X. Tang. Unsupervised learning of discriminative attributes and visual representations. In *CVPR*, 2016.
- [20] A. E. Johnson and M. Hebert. Using spin images for efficient object recognition in cluttered 3d scenes. *IEEE Transactions on pattern analysis and machine intelligence*, 21(5):433–449, 1999.
- [21] A. Karpathy, S. Miller, and L. Fei-Fei. Object discovery in 3d scenes via shape analysis. In *Robotics and Automation (ICRA), 2013 IEEE International Conference on*, pages 2088–2095. IEEE, 2013.
- [22] D. Maturana and S. Scherer. Voxnet: A 3d convolutional neural network for real-time object recognition. In *Intelligent Robots and Systems (IROS), 2015 IEEE/RSJ International Conference on*, pages 922–928. IEEE, 2015.
- [23] C. A. Mueller and A. Birk. Hierarchical graph-based discovery of non-primitive-shaped objects in unstructured environments. In *Robotics and Automation (ICRA), 2016 IEEE International Conference on*, pages 2263–2270. IEEE, 2016.
- [24] P. K. Nathan Silberman, Derek Hoiem and R. Fergus. Indoor segmentation and support inference from rgb-d images. In *ECCV*, 2012.
- [25] J. Papon, A. Abramov, M. Schoeler, and F. Worgotter. Voxel cloud connectivity segmentation-supervoxels for point clouds. In *Proceedings of the IEEE Conference on Computer Vision and Pattern Recognition*, pages 2027–2034, 2013.
- [26] D. Philipona, J. K. O’Regan, and J.-P. Nadal. Is there something out there? inferring space from sensorimotor dependencies. *Neural computation*, 15(9):2029–2049, 2003.
- [27] A. Richtsfeld, T. Mörwald, J. Prankl, M. Zillich, and M. Vincze. Segmentation of unknown objects in indoor environments. In *2012 IEEE/RSJ International Conference on Intelligent Robots and Systems*, pages 4791–4796. IEEE, 2012.
- [28] R. B. Rusu, N. Blodow, and M. Beetz. Fast point feature histograms (fpfh) for 3d registration. In *Robotics and Automation, 2009. ICRA’09. IEEE International Conference on*, pages 3212–3217. IEEE, 2009.
- [29] S. Salti, F. Tombari, and L. Di Stefano. Shot: unique signatures of histograms for surface and texture description. *Computer Vision and Image Understanding*, 125:251–264, 2014.
- [30] F. Schroff, D. Kalenichenko, and J. Philbin. Facenet: A unified embedding for face recognition and clustering. In *CVPR*, 2015.

- [31] G. Sharma and B. Schiele. Scalable nonlinear embeddings for semantic category-based image retrieval. In *ICCV*, 2015.
- [32] J. Shin, R. Triebel, and R. Siegwart. Unsupervised discovery of repetitive objects. In *ICRA*, pages 5041–5046, 2010.
- [33] S. Song and J. Xiao. Deep Sliding Shapes for amodal 3D object detection in RGB-D images. In *CVPR*, 2016.
- [34] F. Tombari, S. Salti, and L. Di Stefano. Unique signatures of histograms for local surface description. In *European conference on computer vision*, pages 356–369. Springer, 2010.
- [35] T. Tuytelaars, C. H. Lampert, M. B. Blaschko, and W. Buntine. Unsupervised object discovery: A comparison. *International journal of computer vision*, 88(2):284–302, 2010.
- [36] A. Wang, J. Lu, J. Cai, T.-J. Cham, and G. Wang. Large-margin multi-modal deep learning for rgb-d object recognition. *IEEE Transactions on Multimedia*, 17(11):1887–1898, 2015.
- [37] X. Wang and A. Gupta. Unsupervised learning of visual representations using videos. In *ICCV*, 2015.
- [38] Z. Wu, S. Song, A. Khosla, F. Yu, L. Zhang, X. Tang, and J. Xiao. 3d shapenets: A deep representation for volumetric shapes. In *Proceedings of the IEEE Conference on Computer Vision and Pattern Recognition*, pages 1912–1920, 2015.
- [39] Q. Zhang, X. Song, X. Shao, H. Zhao, and R. Shibasaki. Unsupervised 3d category discovery and point labeling from a large urban environment. In *Robotics and Automation (ICRA), 2013 IEEE International Conference on*, pages 2685–2692. IEEE, 2013.